An ATP-dependent mechanism mediates intercellular calcium signaling in bone cell network under single cell nanoindentation

Bo Huo [a,d,1], Xin L. Lu [a,1], Kevin D. Costa [b], Qiaobing Xu [c], X. Edward Guo [a,*]

[a] Bone Bioengineering Laboratory, Department of Biomedical Engineering, Columbia University, New York, NY 10027, USA
[b] Cardiac Cell Mechanics Laboratory, Department of Biomedical Engineering, Columbia University, New York, NY 10027, USA
[c] Department of Chemistry and Chemical Biology, Harvard University, Cambridge, MA 02138, USA
[d] Center for Biomechanics and Bioengineering, National Microgravity Laboratory, Institute of Mechanics, Chinese Academy of Sciences, Beijing 100190, PR China

ARTICLE INFO

ABSTRACT

To investigate the roles of intercellular gap junctions and extracellular ATP diffusion in bone cell calcium signaling propagation in bone tissue, *in vitro* bone cell networks were constructed by using microcontact printing and self-assembled monolayer technologies. In the network, neighboring cells were interconnected through functional gap junctions. A single cell at the center of the network was mechanically stimulated by using an AFM nanoindenter. Intracellular calcium ($[Ca^{2+}]_i$) responses of the bone cell network were recorded and analyzed. In the untreated groups, calcium propagation from the stimulated cell to neighboring cells was observed in 40% of the tests. No significant difference was observed in this percentage when the intercellular gap junctions were blocked. This number, however, decreased to 10% in the extracellular ATP-pathway-blocked group. When both the gap junction and ATP pathways were blocked, intercellular calcium waves were abolished. When the intracellular calcium store in ER was depleted, the indented cell can generate calcium transients, but no $[Ca^{2+}]_i$ signal can be propagated to the neighboring cells. No $[Ca^{2+}]_i$ response was detected in the cell network when the extracellular calcium source was removed. These findings identified the biochemical pathways involved in the calcium signaling propagation in bone cell networks.

Published by Elsevier Ltd.

1. Introduction

Mechanical stimuli, such as fluid flow or cell-substrate stretch, can induce intracellular calcium ($[Ca^{2+}]_i$) responses in bone cells [1–3]. It has been shown that the intracellular calcium responses can propagate between neighboring cells and generate an intercellular calcium wave in the bone cell network [4–6]. Intercellular calcium waves have been studied in many cell types, including osteoblastic cells [6–8], glial cells [9], smooth muscle cells [10], kidney cells [11], neurons [12], mast cells [13], and respiratory tracheal ciliated cells [14,15]. For many years, the most intensively investigated mechanism for intercellular calcium wave propagation was based on inositol trisphosphate (IP_3) diffusion through gap junction pores, which triggers calcium release from IP_3-sensitive calcium stores in neighboring cells [15–17]. However, recent studies on glial cells [9], juxtaglomerular cells [11], and two osteoblastic cell lines [7] have shown that intercellular calcium waves can be

propagated between physically separated cells without gap junction communication. In those cells, calcium waves appear to be mediated by the activation of purinergic receptors, presumably by secreted extracellular adenosine triphosphate (ATP). ATP can bind to the membrane-bound P2Y nucleotide receptors, resulting in activation of phospholipase C (PLC), generation of IP_3, and release of intracellular calcium stores [16,17]. Recent evidence revealed that this highly sensitive P2Y receptor/IP_3 signaling pathway might be a faster and more substantial mechanism in mediating the propagation of intercellular calcium waves than the gap junction-dependent pathway [7,12,13,18]. As calcium signaling is essential for bone metabolism and numerous bone cell functions, including proliferation and differentiation [16,17,19–21], information relating to the generation, propagation, and processing mechanisms of intercellular calcium waves in bone cell networks is essential for understanding the behaviors of these cells under different physiological conditions.

Most previous studies on intercellular calcium signaling in various cell types were performed on confluent or sub-confluent cell monolayers. In order to quantitatively evaluate the roles of physical intercellular connections and extracellular messenger diffusion in calcium signal propagation, an *in vitro* cell network with a controlled number of intercellular connections and cell-to-cell distance is more desirable than a monolayer. In our previous study
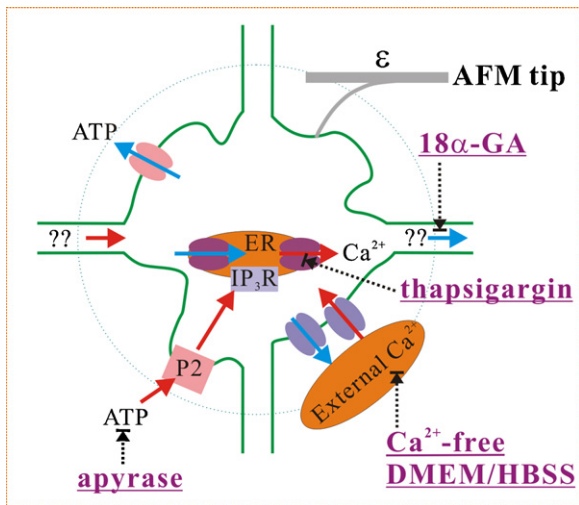
Fig. 1. A schematic of the major calcium signaling pathways involved in bone cells. The corresponding pharmacological agents employed to inhibit or disable these pathways in the present study are illustrated. Red arrow: influx or upregulation activity; Blue arrow: efflux from cytosol; Dash arrow: inhibition or blocking with a specific pharmacological agent. (For interpretation of the references to colour in this figure legend, the reader is referred to the web version of the article.)

[6], a two-dimensional patterned bone cell network was successfully established to mimic the *in vivo* bone cell network by using microcontact printing and self-assembled monolayer (SAM) technologies. Each individual bone cell in the grid network was connected to four neighboring cells via functional gap junctions through uniform distances. When a single cell in the center of the bone network was mechanically stimulated, calcium signal propagation, similar to a point source wave, was observed in the cell network. In our another study, the entire bone cell network was exposed to stimulation by steady fluid flow [3]. Multiple $[Ca^{2+}]_i$ transients, a signature of wave propagation, were observed in the cells. It was also shown that treating the cells with a purinergic receptor antagonist attenuated the $[Ca^{2+}]_i$ response to a single spike. Blocking the intercellular gap junctions, however, had no significant effects on the multiple $[Ca^{2+}]_i$ responses. Therefore, purinergic receptor pathway may play a more critical role than gap junction intercellular communication in the mechanically induced $[Ca^{2+}]_i$ responses in bone cells, given that bone cells express both P2Y receptors and Cx43 gap junction proteins [22,23].

The major purpose of this study was to investigate the dominant propagation mechanism of intercellular calcium waves in bone cell networks. A single cell in the *in vitro* cell network was mechanically stimulated by using an atomic force microscope (AFM) nanoindenter, which enabled us to strictly constrain the stimulation to a single cell and to precisely control the level of applied force [6,24]. The experiments were divided into 8 groups to test the effects of treatment by a battery of pharmacological agents that can interrupt or inhibit different calcium sources and various biochemical signaling pathways. Specifically, we focused on (1) extracellular calcium, (2) intracellular calcium source, (3) direct gap junction intercellular communication, and (4) ATP pathway contributions to calcium wave propagation in bone cell networks (Fig. 1).

2. Materials and methods

2.1. Chemicals

Minimum essential alpha medium (α-MEM), calcium free Dulbecco's modified eagle medium (DMEM), calcium-free Hank's balanced salt solution (HBSS), and DMSO were obtained from Invitrogen Corporation (Carlsbad, CA). Fetal bovine serum (FBS),

charcoal-stripped FBS, and penicillin/streptomycin (P/S) were obtained from Hyclone Laboratories Inc. (Logan, UT). Trypsin/EDTA, octadecanethiol, fibronectin, 18α-glycyrrhetinic acid (18α-GA), apyrase VI (Cat. No. A6410), and thapsigargin were obtained from Sigma–Aldrich Co. (St. Louis, MO). The fluorescent calcium indicator Fluo-4/AM was obtained from Molecular Probes (Carlsbad, CA).

2.2. Bone cell network

Microcontact printing and SAM surface chemistry technologies were employed in the present study to construct the *in vitro* bone cell networks for mechanotransduction experiments [6,25]. To precisely control the geometric topology of the bone cell network, a grid mesh cell pattern was designed (Fig. 2A). The diameter of the round island for a cell to reside was 20 μm. The edge-to-edge distance between neighboring islands was 50 μm. The neighboring islands were connected with 2-μm-width connection lines, through which the cells could build intercellular gap junction connections. These geometric parameters of the pattern have been proved to be optimal for osteoblast-like MC3T3-E1 cells [6]. The designed patterns were first printed on a chromium mask and then replicated to a master made of positive photoresist (Shipley 1818, MicroChem Corp., Newton, MA) by exposing the master to UV light through the chromium mask. Polydimethylsiloxane (PDMS, *Sylgard 184,* Dow Corning, Midland, MI) was poured on the master and cured at 70 °C in an oven for 2 h. A microcontact printing stamp with the designed pattern was obtained by lifting off the PDMS from the surface of master.

MC3T3-E1 cells were cultured in α-MEM containing 10% FBS and 1% P/S and maintained at 37 °C and 5% CO_2 in a humidified incubator. To build a bone cell network with the previously designed pattern, the PDMS stamp was inked with an adhesive SAM (octadecanethiol) and then pressed onto a gold coated glass slide (E-beam evaporator; SC2000, SEMICORE Inc., Livermore, CA). The stamped glass slide was immediately immersed in a non-adhesive ethylene glycol terminated SAM solution (HS-C_{11}-EG_3; Prochimia, Sopot, Poland) for 3 h. A monolayer of EG_3, which can effectively resist protein adsorption and cell adhesion, was formed on areas that were not inked with the adhesive SAM. To further facilitate the cell adhesion on the adhesive SAM inked areas, the glass slide was incubated in a 1% fibronectin solution for 1 h before cell seeding. The fibronectin attached only on the adhesive SAM areas. Finally MC3T3-E1 cells were seeded onto the glass slide (1.0×10^4 cell/cm^2 slide area), and cultured in α-MEM medium with 2% charcoal stripped FBS for at least 24 h before the experiment. In a well-formed cell network (Fig. 2B), each round island was occupied by one cell, and each cell was connected with four neighboring cells through functional gap junctions.

2.3. AFM indentation and $[Ca^{2+}]_i$ responses

To indicate $[Ca^{2+}]_i$ fluctuation, cells in the established network were loaded with 5 μM Fluo-4 AM (Molecular Probes, Eugene, OR) in α-MEM medium with 0.5% charcoal stripped FBS for 1 h in the incubator and then rinsed with fresh medium three times. After Fluo-4 loading, the glass slide was immersed in medium in a Petri dish and placed on an atomic force microscope (AFM; Bioscope, Digital Instruments/Veeco, Santa Barbara, CA), which itself was mounted on the top of an inverted fluorescence microscope (Olympus IX-70). After the Petri dish was secured by vacuum, a 20-min resting period was allowed for the cells to equilibrate to ambient conditions before next step. During the experiment, a single cell at the center of the grid mesh pattern was mechanically stimulated by continuous indenting on the cell surface at 1 Hz frequency for 300 s with an AFM probe. Three different force magnitudes, 30, 60, and 90 nN, were tested to determine an optimal loading
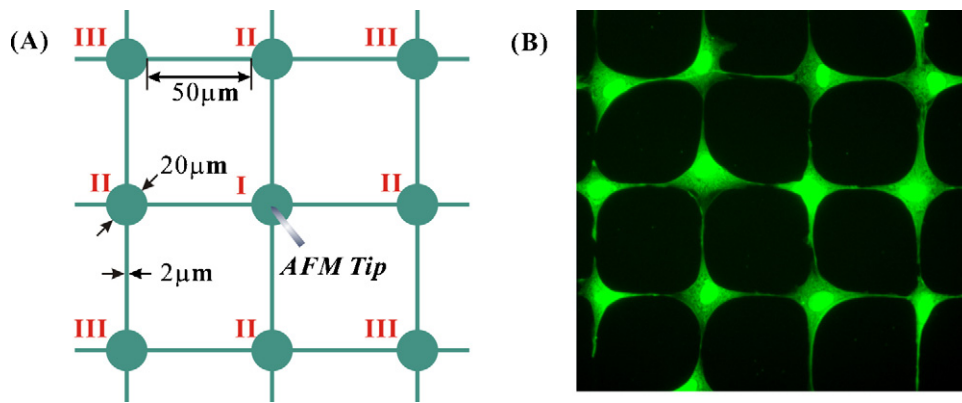
Fig. 2. (A) Schematic of the grid mesh cell pattern designed in this study. All the geometric parameters were specifically optimized for MC3T3-E1 cells. During mechanical stimulation tests, the cell at the center of the grid mesh was indented by an AFM tip. For data analysis, all of the cells were labeled with a Roman numeral according to its distance from the indented cell. (B) Fluorescent image of a typical MC3T3-E1 cell network built on the designed micro-pattern.

level. The indentation was performed using a custom-designed AFM probe with a high aspect ratio, ~150 μm high and 400 μm long (StressedMetal™, Palo Alto Research Center, Palo Alto, CA). This geometric character of the probe minimized the disturbance on the media surrounding the cells [6]. A 20-min resting period before indentation stimulation was sufficient for bone cells to recover from the handling disturbance and to generate repetitive $[Ca^{2+}]_i$ responses [26]. During the experiment, fluorescent images of the cell network were taken every 3 s to record the cell calcium responses by a cooled digital CCD camera (Sensicam, Cooke Corp., Auburn Hills, MI). Image capturing was started 60 seconds before the AFM mechanical stimulation to obtain a baseline of $[Ca^{2+}]_i$ level in each cell, and continued through the entire stimulation process. Recorded images were later analyzed using Metamorph Imaging Software 7.0 (Molecular Devices, Downingtown, PA). The variation of $[Ca^{2+}]_i$ was obtained by measuring the average image intensity of each cell in all time-lapse images.

2.4. Pharmacological agents and experimental groups

Besides the untreated group (17 samples), seven different pharmacological agents were employed to treat the cells before/during experiments in order to identify the sources and the mechanisms of intercellular calcium signaling propagation.

(1) *Vehicle control:* Two of the employed chemicals were dissolved in DMSO. Therefore, a vehicle control group was included with 0.3% v/v DMSO in medium during experiments (10 samples).
(2) *Gap junction blocked:* 75 μM 18α-GA, a reversible gap junction blocker which binds to membrane proteins and causes disassembly of gap junction plaques [27], was supplied in Fluo-4 AM dye medium and remained in medium through the length of the experiment [5] (6 samples).
(3) *ATP blocked:* Apyrase VI, an enzyme that can rapidly hydrolyze extracellular nucleotides, was employed to investigate the effect of extracellular ATP on calcium signal propagation. 10 U/mL apyrase was supplied in the medium 30 min before and during the AFM indentation tests [28] (10 samples).
(4) *Gap junction and ATP blocked*: To simultaneously block gap junctions and the diffusion of extracellular ATP, both 75 μM 18α-GA and 10 U/ml apyrase was added in the medium 30 min before and during the AFM indentation tests (5 samples).
(5) *ER calcium store depleted:* The cell network was incubated in 1 μM thapsigargin medium for 30 min before and during the AFM indentation experiment. Thapsigargin depletes the calcium store inside the endoplasmic reticulum (ER) [3,7,29] (4 samples).

(6) *Extracellular-calcium-depleted:* In this group, after the Fluo-4 AM loading, calcium-free DMEM and calcium-free HBSS were used to replace the regular medium. This treatment removed the extracellular calcium sources immediately before the AFM indentation experiments (5 samples).
(7) *ER calcium store and extracellular-calcium-depleted:* After Fluo-4 staining, the cell-seeded slides were first incubated in 1 μM thapsigargin, and the calcium-free DMEM medium was used through the time of experiment (5 samples).

The selection of the above pharmacological agents and the final employed concentrations were determined based upon the cited literature in bone cell studies. It has been demonstrated that these agents are effective in inhibiting the corresponding pathways in bone cells.

2.5. Data analysis

Each cell in the network was marked with a Roman number according to its distance from the mechanically indented cell, which itself was numbered as cell I. The cell one step away was marked as cell II and so on (Fig. 2A). A cell was defined as responsive to mechanical stimulation if it successfully showed a calcium transient with a magnitude four times larger than its own maximum oscillation during the 60-s baseline measurement period. The percentage of responsive cells for a specific type of cell, *e.g.* cell II, was defined as the number of responsive cells at position II divided by the total number of cell II in the experimental group. The number of responsive neighboring cells for each testing sample was defined as the number of all responsive cells except the indented cell. The average number of responsive neighboring cells in each treated or untreated group was calculated and compared with the other groups treated with pharmacological agents. The magnitudes of $[Ca^{2+}]_i$ spikes were obtained to further investigate the calcium signaling mechanisms.

One-way analysis of variance (ANOVA) with Bonferroni's post hoc analysis was performed to determine statistical differences between different treatments/groups. Statistical significance was indicated when $p < 0.05$. The condition of equal variances of treatment groups was tested by Levene's method.

3. Results

3.1. Typical calcium responses

When the cell in a network was mechanically stimulated, intercellular propagation of calcium signaling to the other cells in the
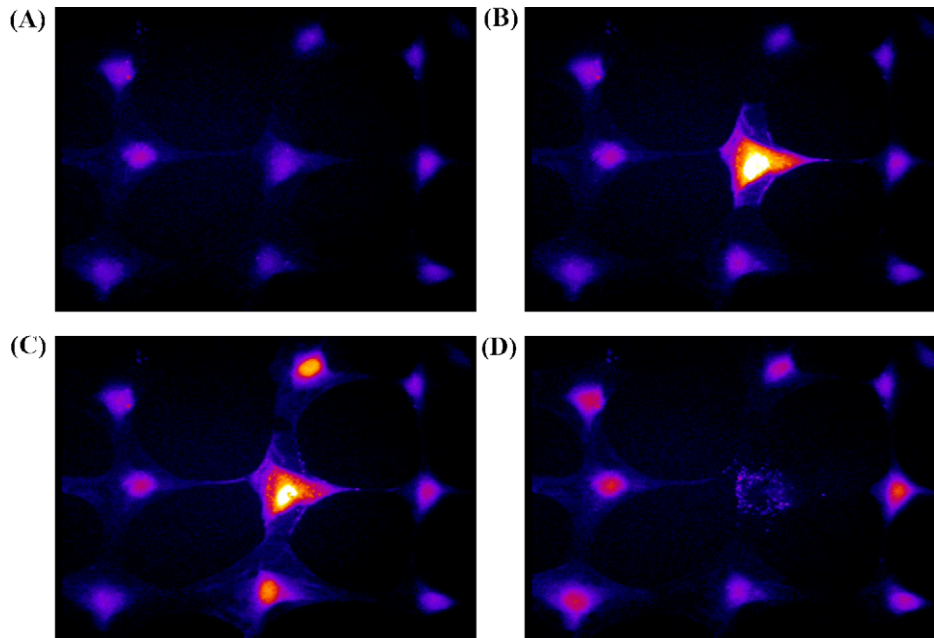
(A)

(B)

(C)

(D)

Fig. 3. Pseudo-color fluorescent images of a typical intercellular calcium signaling process in an MC3T3-E1 cell network (untreated group, ordered in time sequence). This specific test was selected from the 90 nN loading group due to its dramatic $[Ca^{2+}]_i$ oscillations. (A) All the cells showed similar free $[Ca^{2+}]_i$ intensity before stimulation. (B) The cell in the center was mechanically stimulated by an AFM indentation probe. It released a robust calcium spike that reached its peak magnitude in a short time. (C) The calcium signal was propagated to the four neighboring cells (cell II). All cell II showed calcium responses but reached their peak at different time points. (D) The cells two steps away from the indented cell (cell III) showed relatively weaker $[Ca^{2+}]_i$ spikes, while the $[Ca^{2+}]_i$ intensity of the indented cell and cell II have decreased toward to their original levels.

network was clearly observed in most tested samples. Fluorescent images in Fig. 3 showed a typical calcium signal propagation process in the bone cell network. Before an AFM nanoindentation test, all of the cells were stable and had similar $[Ca^{2+}]_i$ intensity (Fig. 3A). The center cell, cell I, was mechanically stimulated at 60 s by the AFM nanoindenter. The $[Ca^{2+}]_i$ intensity of the indented cell increased dramatically in response to the stimulation, as the cell body turned much brighter in the fluorescent images (Fig. 3B). This calcium signal was propagated to the four neighboring cells, cell II. In this specific case, all four cell IIs showed calcium responses with different intensities (Fig. 3C). Later, the calcium signaling was sequentially propagated to cell III (Fig. 3D). From these images, it was also notable that the intensity of $[Ca^{2+}]_i$ responses in the indented cells were usually higher than those of cell II, and the intensity of cell II higher than that of cell III.

3.2. Effect of nanoindentation magnitude

The calcium responses of the bone cell network varied with the magnitude of AFM nanoindentation force (Fig. 4). When the mechanical loading was 30 nN, 83% of the indented cells failed to show any calcium responses to the stimulation. When the force was increased to 60 or 90 nN, however, this number dropped to 15% and 5% respectively. No tested sample showed calcium signaling propagation from the indented cell to its neighboring cells in the 30 nN stimulation group, while 31% and 47.5% tested samples displayed signal propagation in 60 and 90 nN groups. Therefore, the propagation of the intercellular calcium wave depended on the strength of the mechanical stimulation on the source cell. Although the 90 nN force introduced the most dynamic $[Ca^{2+}]_i$ responses and propagations in all the tested samples, a few indented cells (1 out of 5) were observed to burst during the AFM nanoindentation. In the present study, to investigate the mechanisms of the calcium signaling and its intercellular propagation, 60 nN nanoindentation force was adopted for all the other experiments to obtain sufficient $[Ca^{2+}]_i$ responses in the network and to avoid unnecessary cell damage.

3.3. Calcium responses in different groups

The $[Ca^{2+}]_i$ responses in a tested sample can be illustrated by the $[Ca^{2+}]_i$ intensity trace of each individual cell in the network (Fig. 5). To clearly demonstrate the signal propagation process, the typical calcium transients of cell I, cell II, and cell III from a sample were drawn in the plot. In all of the tested groups other than the extracellular-calcium-depleted group, a prominent $[Ca^{2+}]_i$ responsive peak in the stimulated cell (cell I) was observed immediately after the start of AFM nanoindentation. Although the
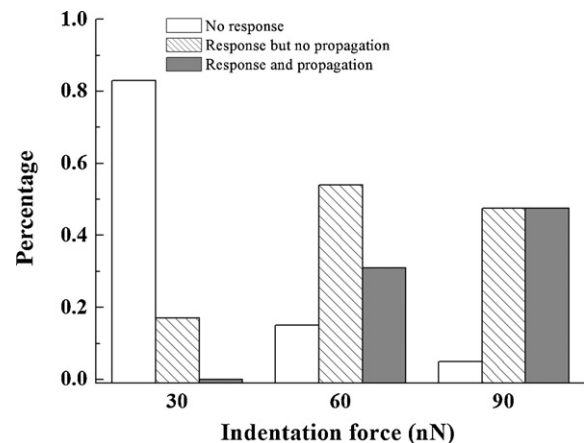

Fig. 4. Different magnitudes of the AFM indentation force generated different calcium responses in the bone cell network. The tested samples at each force level were separated into three groups based on their calcium responses. "No response" refers to mechanically stimulated cells that had no observed $[Ca^{2+}]_i$ response. 'Response but no propagation' refers to mechanically stimulated cell showed $[Ca^{2+}]_i$ transients, but all the other cells have no responses. 'Response and propagation' indicates that both the stimulated cell and the neighboring cells in the network displayed $[Ca^{2+}]_i$ waves. The sample numbers for the indentation forces of 30, 60 and 90 nN are 6, 13 and 40, respectively.
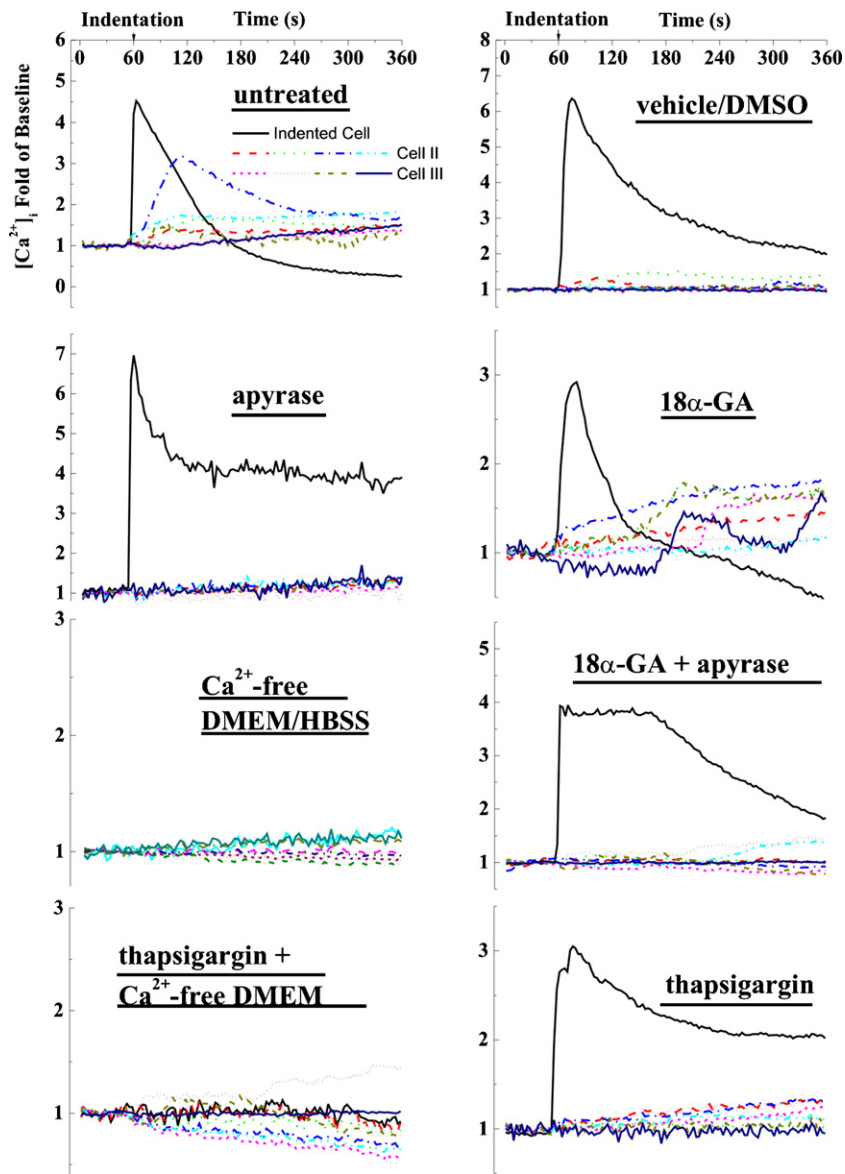
Fig. 5. A set of typical intracellular calcium traces of indented cell, cell II, and cell III for all experimental groups. The calcium responses were recorded for 6 min:1 min for baseline and 5 min during mechanical stimulation. The $[Ca^{2+}]_i$ intensity was represented by the cell image intensity normalized by the average baseline level.

mechanical stimulation was applied on cell I throughout the entire experiment, the $[Ca^{2+}]_i$ intensity of cell I decreased slowly after reaching the first peak. The neighboring cells, cell II and cell III, also showed $[Ca^{2+}]_i$ waves in the untreated, vehicle control, and gap-junction-blocked groups. The magnitude of the $[Ca^{2+}]_i$ peak of the neighboring cells, however, were much lower than those of the indented cells, especially for the vehicle control group. The calcium signal propagation was barely observed in the ATP-blocked group, ER calcium-store-depleted group and the gap-junction-and-ATP-blocked group, although the indented cell in these three groups showed normal $[Ca^{2+}]_i$ responses. Interestingly, when the extracellular medium was free of calcium, none of the cells in the network, even the directly indented one, was able to generate calcium responses to mechanical stimulation.

3.4. Propagation of calcium signaling

The average number of responsive neighboring cells for different groups are shown and compared in Fig. 6. This number was counted as zero for tested samples without signal propagation. The aver-

age number of responsive neighboring cells in the untreated group was 1.7 ± 0.24, without significant difference with the vehicle control group (2.2 ± 0.4). The gap-junction-blocked group (1.8 ± 0.6) was not significantly different with the untreated or vehicle control group. The ATP-blocked group (apyrase) had a significantly lower number of responsive neighboring cells (0.4 ± 0.2). The ER-calcium-store-depleted (thapsigargin) group and the gap-junction-and-ATP-blocked (apyrase/thapsigargin) group had no responsive neighboring cells except the indented one. The percentages of responsive cells of cell II and cell III were compared between different treatment groups (Fig. 7). 30–50% of cell II showed $[Ca^{2+}]_i$ responses in the untreated, vehicle control, and gap-junction-blocked groups, and no significant difference was detected between these three groups. The percentage of responsive cell II in these three groups, however, was significantly higher than those of the ATP-blocked group and ER-calcium-store-depleted group, which are 9% and 0% respectively. The percentage of responsive cell III was significantly lower than that of cell II. Only 9% of cell III in the untreated group were responsive, which has no significant difference with the vehicle control group (25%) and gap-junction-
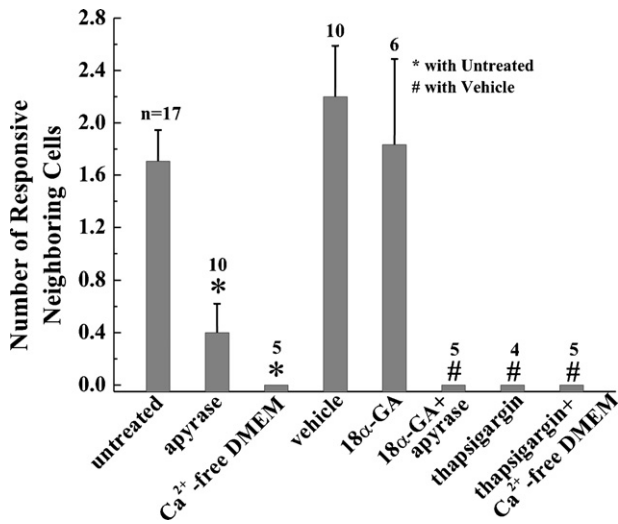
Fig. 6. The average number of responsive neighboring cells for all pharmacologically treated groups. The error bars are SEM while * indicates statistical significance of $p < 0.05$ with the untreated group and # indicates statistical significance of $p < 0.05$ with vehicle (DMSO) control group. The numbers above data bars indicate the n number of experiments.

blocked group (10%). 3% of cell III in the ATP-blocked group were responsive. The ER-calcium-store-depleted group had no responsive cell III. However, due to the small sample size here, an ANOVA was unable to be performed to compare the responses of cell III between different groups. Again, neither cell II nor cell III responded in the two extracellular-calcium-depleted groups.

Although apyrase treatment significantly impeded the propagation of intercellular calcium waves, the peak magnitudes of $[Ca^{2+}]_i$ transient in responsive cells were not affected when compared with the untreated group (Fig. 8). The peak magnitudes of $[Ca^{2+}]_i$ transients of the indented cell (Fig. 8A) and cell II (B) in the ATP-blocked group were same as those of the untreated group. For the indented cells, blocking the intercellular gap junctions using 18α-GA had no effect on the peak magnitude. This phenomenon was further confirmed by the results from the gap-junction-and-ATP-blocked group, which showed no significant difference with the vehicle control group. When the calcium store in the ER was depleted by thapsigargin, the magnitude of $[Ca^{2+}]_i$ transients in the indented cells was not different from that of the vehicle control group. In the two ER-calcium-store-depleted groups and the gap-junction-and-
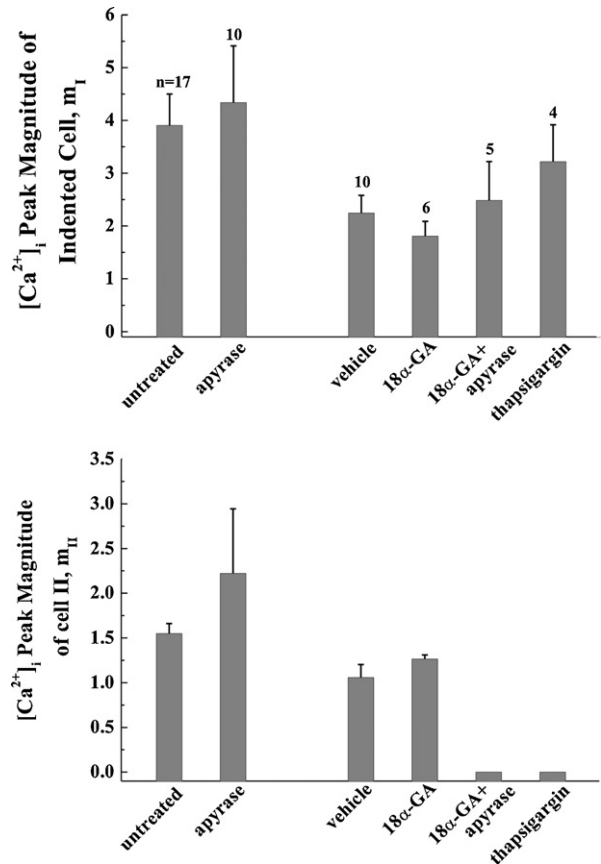
Fig. 8. The magnitude of $[Ca^{2+}]_i$ peak for (A) the indented cell and (B) cell II. The apyrase-treated group was compared with the untreated group. Since DMSO was used in all the other groups, the results from these groups were compared with the vehicle (DMSO) control group. The numbers above data bars indicate the n number of experiments. The n numbers are the same for the indented cell and cell II.

ATP-blocked group, the calcium wave was interrupted, and there were no calcium responses in cell II (Fig. 8B). There was no significant difference in the peak magnitudes of responsive cell II in the gap-junction-blocked group and the vehicle control group.

4. Discussion

Increases in $[Ca^{2+}]_i$ concentration that spread from cell to cell provide a mechanism for bone cells to coordinate many cellular activities. In this study, we investigated the mechanism implicated in the propagation of intercellular calcium signals in MC3T3-E1 osteoblast-like cells. Gap junction communication has long been conjectured to be a major candidate for this intercellular signal propagation. Nonetheless, recent studies have demonstrated that ATP was an important extracellular messenger in calcium waves of many cell types [7,9,11,13,30]. Since both the P2Y class of purinergic receptors and the gap junction protein Cx43 have been well-characterized in MC3T3-E1 osteoblastic cells, specific inhibitors interfering with both pathways were employed here to determine their relative importance to calcium intercellular signal propagation. We found that calcium wave propagation was significantly impeded when extracellular ATP was hydrolyzed by apyrase. Chemical blocking of gap junctions did not impair the calcium wave propagations, suggesting that the diffusion of IP₃ or $[Ca^{2+}]_i$ through gap junction pores is unlikely to be a major contributor to calcium wave propagation. It is therefore ATP, rather than gap junction channels, that dominantly mediates the transmission of mechanically elicited intercellular calcium signaling in MC3T3-E1 cells. This
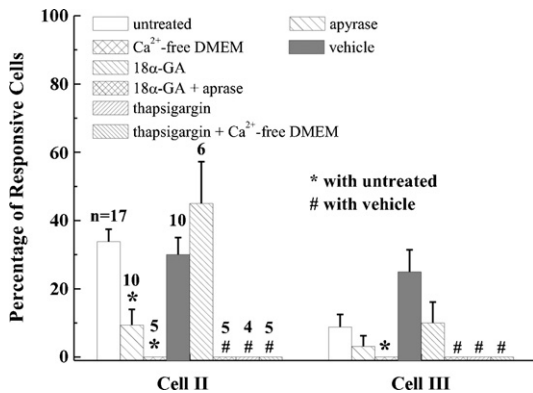

Fig. 7. The percentage of responsive cells for cell II (one step away from the indented cell) and cell III (two steps away from the indented cell) in different groups. The error bars are standard errors of the means (SEM) while * indicates statistical significance of $p < 0.05$ with the untreated group and # indicates statistical significance of $p < 0.05$ with vehicle (DMSO) control group. The numbers above data bars indicate the n number of experiments. The n numbers are the same for cell II and cell III.

observation is in line with those previously reported for rat mast cells [13], hepatocytes [31,32], osteoblastic cell lines [7,30], pancreatic beta cells [33], C6 glioma cells [34], glial cells [9], Hela cells [35] and U373 glioblastoma cells.

In this study we induced intercellular calcium waves by nanoindenting a single cell with a custom-designed AFM probe. Unlike the glass micropipette used in most previous studies, the loading strength and frequency can be precisely controlled by using an AFM probe. It has been shown that higher mechanical stress was significantly more stimulatory to bone cells [36]. By using different indenting forces, 30, 60, and 90 nN, our results confirmed that both percentage of responsive cells and the intensity of $[Ca^{2+}]_i$ response were dependent on the stimulation force. Thus, it is important to unify the mechanical parameters in future mechanotransduction tests in order to compare the outputs from different experimental groups.

The molecular mechanisms of ATP release are still a matter of debate. It has been shown that osteoblastic cells contain stretch-activated cation channels [37]. Non-voltage-dependent, stretch-sensitive channels are involved in the mechanically induced Ca^{2+} influx, which induce ATP release. Later studies on MC3T3-E1 cells showed that fluid shear can activate L-type voltage-sensitive Ca^{2+} channels on the membrane to promote Ca^{2+} entry that, in turn, stimulates vesicular ATP release [38,39]. Both studies pointed toward the fact that release of ATP requires Ca^{2+} influx. In this study, mechanical nanoindentation failed to initiate any $[Ca^{2+}]_i$ responses in either the stimulated cells or neighboring cells when calcium-free medium was used. A similar result was observed in our fluid flow study on MC3T3-E1 networks [3]. The $[Ca^{2+}]_i$ responses in neighboring cells with an intracellular calcium response were mainly induced through the purinergic receptor pathway by extracellular ATP diffused from the indented cell. In the present study, intercellular calcium waves of a finite distance were observed in the MC3T3-E1 cell network. The intensity of $[Ca^{2+}]_i$ responses decreased as the signaling wave spread from cell to cell. In most of the untreated tests, the $[Ca^{2+}]_i$ responses vanished at cells two steps away from the stimulated cell. However, this does not rule out the possibility that there was a sequential release of ATP by cells along the path of the calcium wave. Since the calcium wave is diminishing along the propagation direction, the ATP released from neighboring cells could be markedly lower than that from the indented cell.

Extracellular ATP possesses all the properties of a fast-acting intercellular messenger. It is released in a controlled fashion, ligates specific plasma membrane receptors coupled to signal transduction, and quickly degrades to terminate its actions. Although the present study demonstrates a significant role for ATP in MC3T3-E1 calcium wave propagation, the findings did not rule out the involvement of IP_3 or other second messengers that can diffuse through gap junction pores. Our results showed that treatment with apyrase alone did not completely abolish calcium signal propagation. When 18α-GA was employed together with apyrase for cell treatment, the intercellular calcium wave vanished. Treatment with 18α-GA alone, however, had no significant effect on calcium wave propagation. Therefore the results from different groups indicated that propagation of second messengers through gap junction pores still existed and might have assisted the propagation of calcium waves in the MC3T3-E1 cell network. This could easily be overshadowed by the sensitive and fast purinergic receptor pathway. Previous studies on another osteoblast cell line have also shown that the calcium wave through gap junction communication is slow and weak [7].

Calcium signal propagation has been previously investigated in two other rat osteosarcoma/osteoblastic cell lines, UMR 106-01 cells and ROS 17/2.8 [7]. It was found that a single UMR cell in a monolayer stimulated by a pipette can spread the calcium wave to 30–50 surrounding cells in a few seconds via an ATP signaling pathway. Stimulation of a single ROS cell, however, generates strikingly slow calcium waves within only a few neighboring cells, which are shown to be dependent on gap junction communication and influx of extracellular calcium via voltage-gated calcium channels. Taken together with our present findings with MC3T3-E1 cells, it is clear that the propagation mechanisms of intercellular calcium wave in osteoblastic cells are cell-line dependent. Immunofluorescence with antibodies to Cx43 revealed that ROS 17/2.8 expressed more Cx43 proteins than MC3T3-E1 or UMR 106 cells [22]. UMR and MC3T3-E1 express P2Y receptors in the membrane, but ROS cells do not. It seems that these diversities extend to the mechanisms underlying calcium wave propagations. This finding may have important implications to the study of calcium signaling in different types of cells or cell lines.

Current experimental results from extracellular-calcium-depleted and ER-calcium-store-depleted groups have identified the calcium sources underlying the $[Ca^{2+}]_i$ responses in MC3T3-E1 cells. Cells in calcium-free medium showed no response to either fluid flow or AFM nanoindentation stimulations. This implicated that the $[Ca^{2+}]_i$ transients in MC3T3-E1 cells induced by mechanical stimulation have to be initiated with extracellular calcium influx. Literature has shown that the role of extracellular calcium in $[Ca^{2+}]_i$ responses are cell line and type dependent. A few researchers noted that the influx of extracellular calcium is required to evoke the opening of the calcium release channels in the ER [40,41], while studies on the ROS 17/2.8 cell line and human prostate cancer cells showed that extracellular calcium was not necessary for calcium wave propagation [42,43]. Another major calcium source for $[Ca^{2+}]_i$ responses is the intracellular calcium store, which is mainly held within the membrane systems of the ER [44,45]. Extracellular ATP can activate the purinergic receptors of the G protein-coupled P2Y class that activate phospholipase C, resulting in the generation of IP_3 and intracellular calcium release from IP_3-sensitive ER calcium stores. In this study, depletion of the ER stores with thapsigargin severely hampered intercellular calcium signaling, although the indented cell showed normal responses. Experiments on MC3T3-E1 monolayer (results not shown) demonstrated that exogenous application of ATP can barely induce $[Ca^{2+}]_i$ responses when the ER Ca^{2+} store was depleted, but the response did not require the extracellular Ca^{2+} source. Therefore the calcium response of neighboring cells to ATP is mostly due to the ER calcium release and does not require the extracellular calcium influx. When the ER store was depleted by thapsigargin, the neighboring cells failed to release $[Ca^{2+}]_i$ transients with calcium-depleted ER.

Certain limitations should be emphasized regarding the present study. First, the pharmacological agents employed in the pathway-inhibition studies may have side-effect on cell activities and further affect the calcium responses. It has been noticed that the treatment of 18α-GA on MC3T3-E1 cells changed the time course of $[Ca^{2+}]_i$ transients[3]. Second, it has been shown that osteoblast interactions with extracellular matrix (ECM) proteins can influence many cell functions, which may affect the calcium signaling of the cells. The choice of fibronectin in present study is based on the findings of our previous work, which has shown that fibronectin-coated substrate provided better adhesion, FAK activation, and more PGE_2 release for MC3T3-E1 cells [46]. However, the calcium responses of cells may vary if other substrates were used. Third, it was found that ATP activation of P2Y receptors can activate protein kinase C, the activation of which may partially affect the $[Ca^{2+}]_i$ responses of cells [47]. Despite the above limitations, the major conclusions obtained in the present study, as consistent with most previously reported results for other types of cells, appear to be valid and provide additional and valuable insight for the mechanisms of calcium wave propagations in bone cell networks.

Acknowledgment

References

[1] A. Liedert, D. Kaspar, R. Blakytny, L. Claes, A. Ignatius, Signal transduction pathways involved in mechanotransduction in bone cells, Biochem. Biophys. Res. Commun. 349 (2006) 1–5.

[2] J. Rubin, C. Rubin, C.R. Jacobs, Molecular pathways mediating mechanical signaling in bone, Gene 367 (2006) 1–16.

[3] B. Huo, X.L. Lu, C.T. Hung, K.D. Costa, Q.B. Xu, G.M. Whitesides, X.E. Guo, Fluid flow induced calcium response in bone cell network, Cell. Mol. Bioeng. 1 (2008) 58–66.

[4] S.L. Xia, J. Ferrier, Propagation of a calcium pulse between osteoblastic cells, Biochem. Biophys. Res. Commun. 186 (1992) 1212–1219.

[5] C.E. Yellowley, Z. Li, Z. Zhou, C.R. Jacobs, H.J. Donahue, Functional gap junctions between osteocytic and osteoblastic cells, J. Bone Miner. Res. 15 (2000) 209–217.

[6] X.E. Guo, E. Takai, X. Jiang, Q. Xu, G.M. Whitesides, J.T. Yardley, C.T. Hung, E.M. Chow, T. Hantschel, K.D. Costa, Intracellular calcium waves in bone cell networks under single cell nanoindentation, Mol. Cell Biomech. 3 (2006) 95–107.

[7] N.R. Jorgensen, S.T. Geist, R. Civitelli, T.H. Steinberg, ATP- and gap junction-dependent intercellular calcium signaling in osteoblastic cells, J. Cell Biol. 139 (1997) 497–506.

[8] P. Gomez, J. Vereecke, B. Himpens, Intra- and intercellular $Ca^{(2+)}$-transient propagation in normal and high glucose solutions in ROS cells during mechanical stimulation, Cell Calcium 29 (2001) 137–148.

[9] P.B. Guthrie, J. Knappenberger, M. Segal, M.V. Bennett, A.C. Charles, S.B. Kater, ATP released from astrocytes mediates glial calcium waves, J. Neurosci. 19 (1999) 520–528.

[10] M. Fanchaouy, K. Serir, J.J. Meister, J.L. Beny, R. Bychkov, Intercellular communication: role of gap junctions in establishing the pattern of ATP-elicited Ca^{2+} oscillations and Ca^{2+}-dependent currents in freshly isolated aortic smooth muscle cells, Cell Calcium 37 (2005) 25–34.

[11] J. Yao, M. Suwa, B. Li, K. Kawamura, T. Morioka, T. Oite, ATP-dependent mechanism for coordination of intercellular Ca^{2+} signaling and renin secretion in rat juxtaglomerular cells, Circ. Res. 93 (2003) 338–345.

[12] Y. Zeng, X.H. Lv, S.Q. Zeng, S.L. Tian, M. Li, J. Shi, Sustained depolarization-induced propagation of $[Ca^{(2+)}]_{(i)}$ oscillations in cultured DRG neurons: the involvement of extracellular ATP and P2Y receptor activation, Brain Res. 1239 (2008) 12–23.

[13] Y. Osipchuk, M. Cahalan, Cell-to-cell spread of calcium signals mediated by ATP receptors in mast cells, Nature 359 (1992) 241–244.

[14] M.J. Sanderson, A.C. Charles, E.R. Dirksen, Mechanical stimulation and intercellular communication increases intracellular Ca^{2+} in epithelial cells, Cell Regul. 1 (1990) 585–596.

[15] S. Boitano, E.R. Dirksen, M.J. Sanderson, Intercellular propagation of calcium waves mediated by inositol trisphosphate, Science 258 (1992) 292–295.

[16] M.J. Berridge, P. Lipp, M.D. Bootman, The versatility and universality of calcium signalling, Nat. Rev. Mol. Cell Biol. 1 (2000) 11–21.

[17] J. Iqbal, M. Zaidi, Molecular regulation of mechanotransduction, Biochem. Biophys. Res. Commun. 328 (2005) 751–755.

[18] N.R. Jorgensen, Short-range intercellular calcium signaling in bone, APMIS Suppl (2005) 5–36.

[19] M. Zayzafoon, K. Fulzele, J.M. McDonald, Calmodulin and calmodulin-dependent kinase IIα regulate osteoblast differentiation by controlling c-fos expression, J. Biol. Chem. 280 (2005) 7049–7059.

[20] K. Sato, A. Suematsu, T. Nakashima, S. Takemoto-Kimura, K. Aoki, Y. Morishita, H. Asahara, K. Ohya, A. Yamaguchi, T. Takai, T. Kodama, T.A. Chatila, H. Bito, H. Takayanagi, Regulation of osteoclast differentiation and function by the CaMK–CREB pathway, Nat. Med. 12 (2006) 1410–1416.

[21] M. Zayzafoon, Calcium/calmodulin signaling controls osteoblast growth and differentiation, J. Cell Biochem. 97 (2006) 56–70.

[22] H.J. Donahue, K.J. McLeod, C.T. Rubin, J. Andersen, E.A. Grine, E.L. Hertzberg, P.R. Brink, Cell-to-cell communication in osteoblastic networks: cell line-dependent hormonal regulation of gap junction function, J. Bone Miner. Res. 10 (1995) 881–889.

[23] J. You, C.R. Jacobs, T.H. Steinberg, H.J. Donahue, P2Y purinoceptors are responsible for oscillatory fluid flow-induced intracellular calcium mobilization in osteoblastic cells, J. Biol. Chem. 277 (2002) 48724–48729.

[24] G.T. Charras, P.P. Lehenkari, M.A. Horton, Atomic force microscopy can be used to mechanically stimulate osteoblasts and evaluate cellular strain distributions, Ultramicroscopy 86 (2001) 85–95.

[25] R. Singhvi, A. Kumar, G.P. Lopez, G.N. Stephanopoulos, D.I. Wang, G.M. Whitesides, D.E. Ingber, Engineering cell shape and function, Science 264 (1994) 696–698.

[26] L.M. Godin, S. Suzuki, C.R. Jacobs, H.J. Donahue, S.W. Donahue, Mechanically induced intracellular calcium waves in osteoblasts demonstrate calcium fingerprints in bone cell mechanotransduction, Biomech. Model Mechanobiol. 6 (2007) 391–398.

[27] Y. Guo, C. Martinez-Williams, K.A. Gilbert, D.E. Rannels, Inhibition of gap junction communication in alveolar epithelial cells by 18α-glycyrrhetinic acid, Am. J. Physiol. 276 (1999) L1018–1026.

[28] R.C. Riddle, A.F. Taylor, J.R. Rogers, H.J. Donahue, ATP release mediates fluid flow-induced proliferation of human bone marrow stromal cells, J. Bone Miner. Res. 22 (2007) 589–600.

[29] C.T. Hung, F.D. Allen, K.D. Mansfield, I.M. Shapiro, Extracellular ATP modulates $[Ca^{2+}]_i$ in retinoic acid-treated embryonic chondrocytes, Am. J. Physiol. 272 (1997) C1611–1617.

[30] Z. Henriksen, J.F. Hiken, T.H. Steinberg, N.R. Jorgensen, The predominant mechanism of intercellular calcium wave propagation changes during long-term culture of human osteoblast-like cells, Cell Calcium 39 (2006) 435–444.

[31] M.H. Nathanson, S.F. Schlosser, Calcium signaling mechanisms in liver in health and disease, Prog. Liver Dis. 14 (1996) 1–27.

[32] C. Clair, C. Chalumeau, T. Tordjmann, J. Poggioli, C. Erneux, G. Dupont, L. Combettes, Investigation of the roles of $Ca^{(2+)}$ and $InsP_{(3)}$ diffusion in the coordination of $Ca^{(2+)}$ signals between connected hepatocytes, J. Cell Sci. 114 (2001) 1999–2007.

[33] D. Cao, G. Lin, E.M. Westphale, E.C. Beyer, T.H. Steinberg, Mechanisms for the coordination of intercellular calcium signaling in insulin-secreting cells, J. Cell Sci. 110 (Pt 4) (1997) 497–504.

[34] T. Fry, J.H. Evans, M.J. Sanderson, Propagation of intercellular calcium waves in C6 glioma cells transfected with connexins 43 or 32, Microsc. Res. Tech. 52 (2001) 289–300.

[35] G.C. Lin, J.K. Rurangirwa, M. Koval, T.H. Steinberg, Gap junctional communication modulates agonist-induced calcium oscillations in transfected HeLa cells, J. Cell Sci. 117 (2004) 881–887.

[36] S.W. Donahue, C.R. Jacobs, H.J. Donahue, Flow-induced calcium oscillations in rat osteoblasts are age, loading frequency, and shear stress dependent, Am. J. Physiol. Cell Physiol. 281 (2001) C1635–1641.

[37] N Kizer, X.L. Guo, K. Hruska, Reconstitution of stretch-activated cation channels by expression of the α-subunit of the epithelial sodium channel cloned from osteoblasts, Proc. Natl. Acad. Sci. U.S.A. 94 (1997) 1013–1018.

[38] D.C. Genetos, D.J. Geist, D. Liu, H.J. Donahue, R.L. Duncan, Fluid shear-induced ATP secretion mediates prostaglandin release in MC3T3-E1 osteoblasts, J. Bone Miner. Res. 20 (2005) 41–49.

[39] D.C. Genetos, C.J. Kephart, Y. Zhang, C.E. Yellowley, H.J. Donahue, Oscillating fluid flow activation of gap junction hemichannels induces ATP release from MLO-Y4 osteocytes, J. Cell Physiol. 212 (2007) 207–214.

[40] H. Mogami, A.V. Tepikin, O.H. Petersen, Termination of cytosolic Ca^{2+} signals: Ca^{2+} reuptake into intracellular stores is regulated by the free Ca^{2+} concentration in the store lumen, Embo J. 17 (1998) 435–442.

[41] N.R. Jorgensen, S.C. Teilmann, Z. Henriksen, R. Civitelli, O.H. Sorensen, T.H. Steinberg, Activation of L-type calcium channels is required for gap junction-mediated intercellular calcium signaling in osteoblastic cells, J. Biol. Chem. 278 (2003) 4082–4086.

[42] H. Sauer, J. Hescheler, M. Wartenberg, Mechanical strain-induced $Ca^{(2+)}$ waves are propagated via ATP release and purinergic receptor activation, Am. J. Physiol. Cell Physiol. 279 (2000) C295–307.

[43] S. Katz, R. Boland, G. Santillan, Modulation of ERK 1/2 and p38 MAPK signaling pathways by ATP in osteoblasts: involvement of mechanical stress-activated calcium influx, PKC and Src activation, Int. J. Biochem. Cell Biol. 38 (2006) 2082–2091.

[44] M.J. Berridge, Inositol trisphosphate and calcium signalling, Nature 361 (1993) 315–325.

[45] D.E. Clapham, Calcium signaling, Cell 80 (1995) 259–268.

[46] E. Takai, R. Landesberg, R.W. Katz, C.T. Hung, X.E. Guo, Substrate modulation of osteoblast adhesion strength, focal adhesion kinase activation, and responsiveness to mechanical stimuli, Mol. Cell Biomech. 3 (2006) 1–12.

[47] V.P Fomin, A. Kronbergs, S. Gunst, D. Tang, V. Simirskii, M. Hoffman, R.L. Duncan, Role of protein kinase Cα in regulation of $[Ca^{2+}]_i$ and force in human myometrium, Reprod. Sci. 16 (2009) 71–79.